Figures and figure supplements

Embryonic origin and serial homology of gill arches and paired fins in the skate, *Leucoraja erinacea*

Victoria A Sleight and J Andrew Gillis

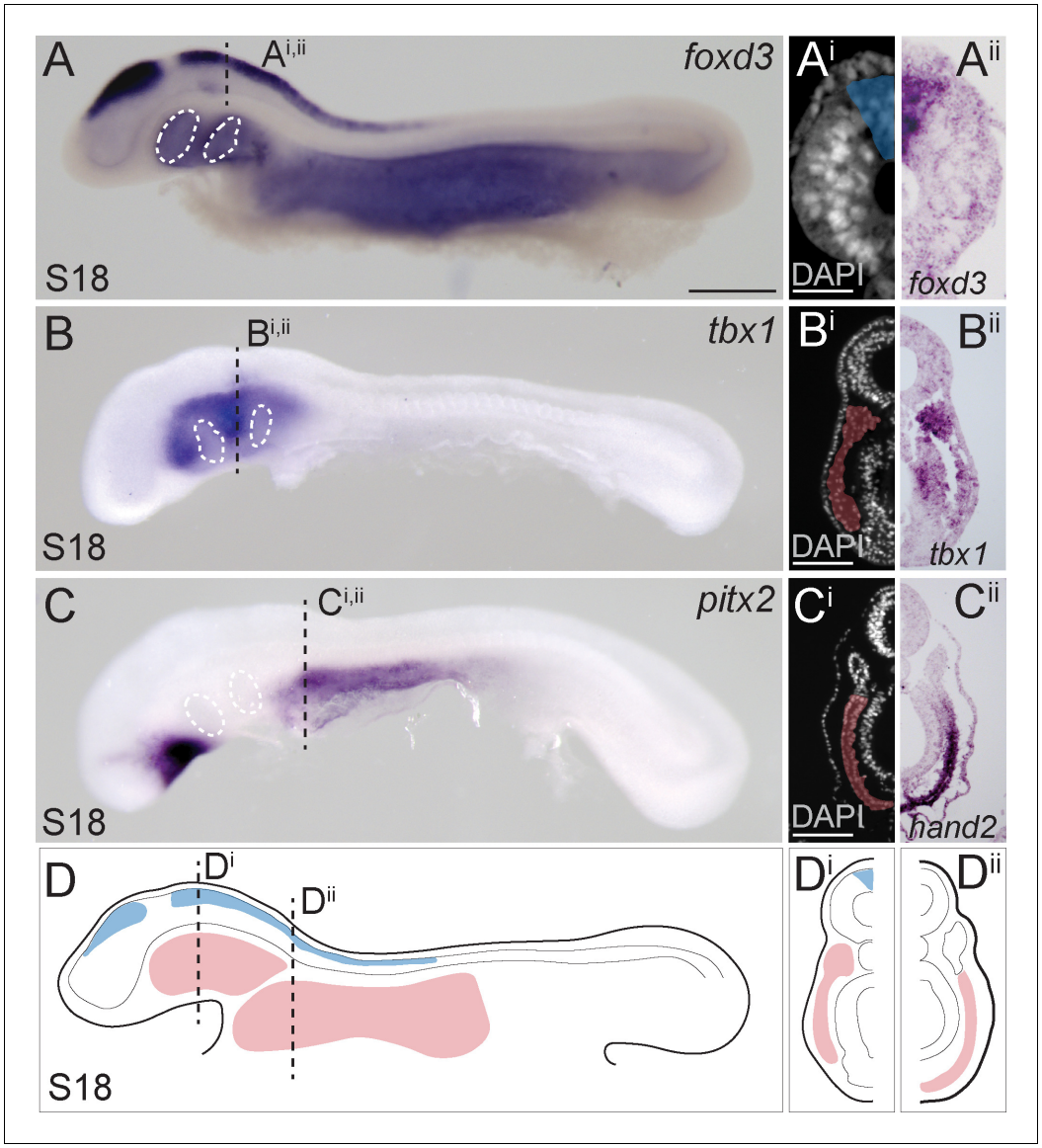

Figure 1. Neural crest and mesoderm after skate neurulation. (**A**) Wholemount mRNA in situ hybridization for *foxD3* reveals expression in (**Ai, Aii**) pre-migratory neural crest cells within the dorsal neural tube of the skate embryo at S18. (**B, Bi, Bii**) *tbx1*-expressing head mesoderm grades into (**C**) *pitx2*- and (**Ci, Cii**) *hand2*-expressing lateral plate mesoderm in the skate embryo at S18. (**D**) Schematic representation of neural crest, head mesoderm and lateral plate mesoderm tissues targeted for cell lineage tracing in this study. White dashed lines indicate the location of developing pharyngeal endodermal pouches. Scale bars: (**A**, **B**), C = 700 µm; A^i = 65 µm; (B^i), C^i = 120 µm.

Figure 1—figure supplement 1. Paraxial mesoderm in the little skate. (**A**) Wholemount mRNA in situ hybridization for *myf5* reveals expression in (**Ai, Aii**) somitic and presomitic mesoderm of the skate embryo at S18.

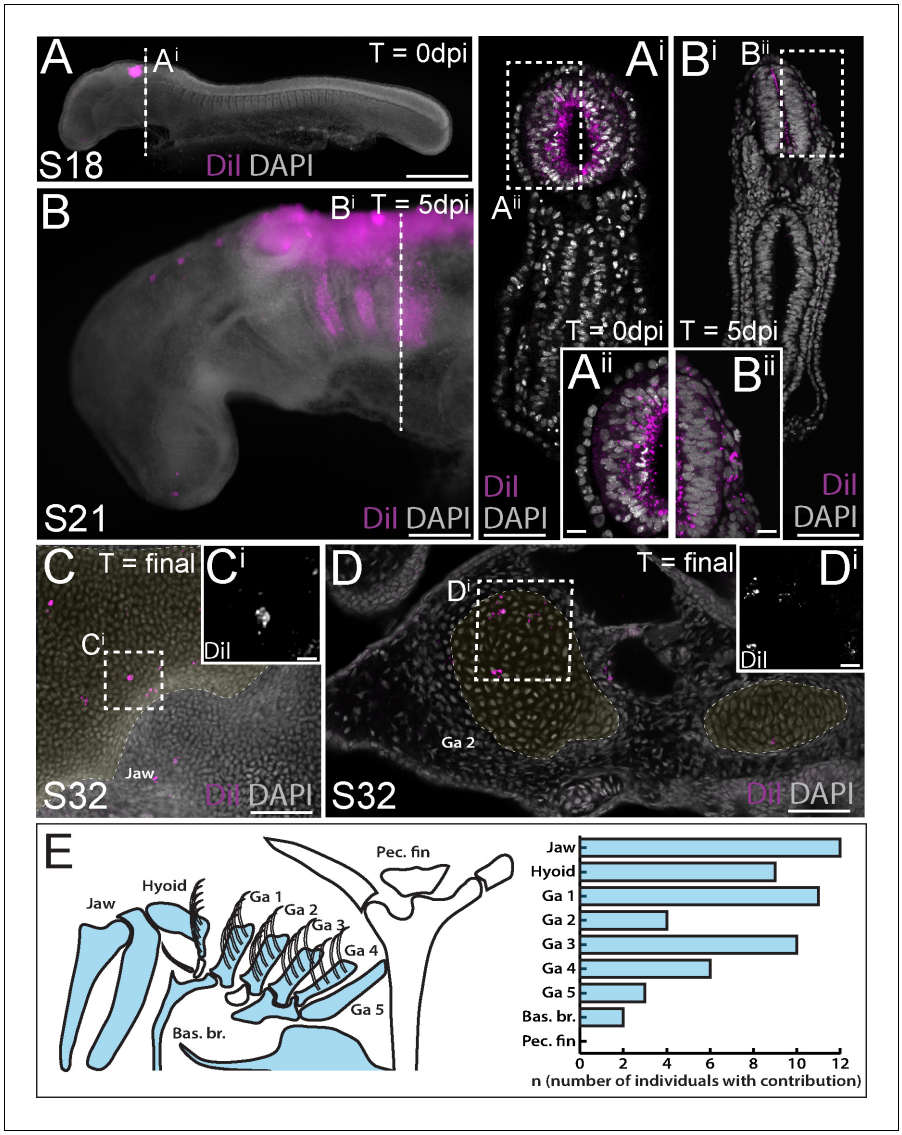

Figure 2. Neural crest contributes to the jaw, hyoid and gill arch skeleton in the skate. (**A**) Microinjection of CM-DiI into the lumen of the neural tube at S18 results in (**A^{i}**, **Aii**) labelling of cells throughout the hindbrain neural tube, including premigratory neural crest cells. (**B**) At 5 days post-injection (dpi), CM-DiI-labelled cranial neural crest cells can be seen streaming from the hindbrain neural tube into the pharyngeal arches (see also **B^{i}**, **B^{ii}**). At S32, CM-DiI (i.e. neural crest-derived) chondrocytes are recovered within pharyngeal arch skeletal elements, including (**C**, **C^{i}**) the palatoquadrate of the jaw and (**D**, **Di**) the epibranchial of gill arch 2. (**E**) Schematic representation of pharyngeal and pectoral fin skeletal elements in the S32 skate embryo, with elements receiving contribution from neural crest coloured blue, and a plot showing the number of embryos observed with neural crest contributions to the pharyngeal arch skeleton. In (**C** and **D**), cartilaginous elements are false-coloured yellow. Scale bars: A = 700 µm; A^{i} = 250 µm; A^{ii} = 50 µm; B = 340 µm; B^{i} = 250 µm; B^{ii} = 50 µm; C = 165 µm; C^{i} = 15 µm; D = 70 µm; D^{i} = 20 µm.

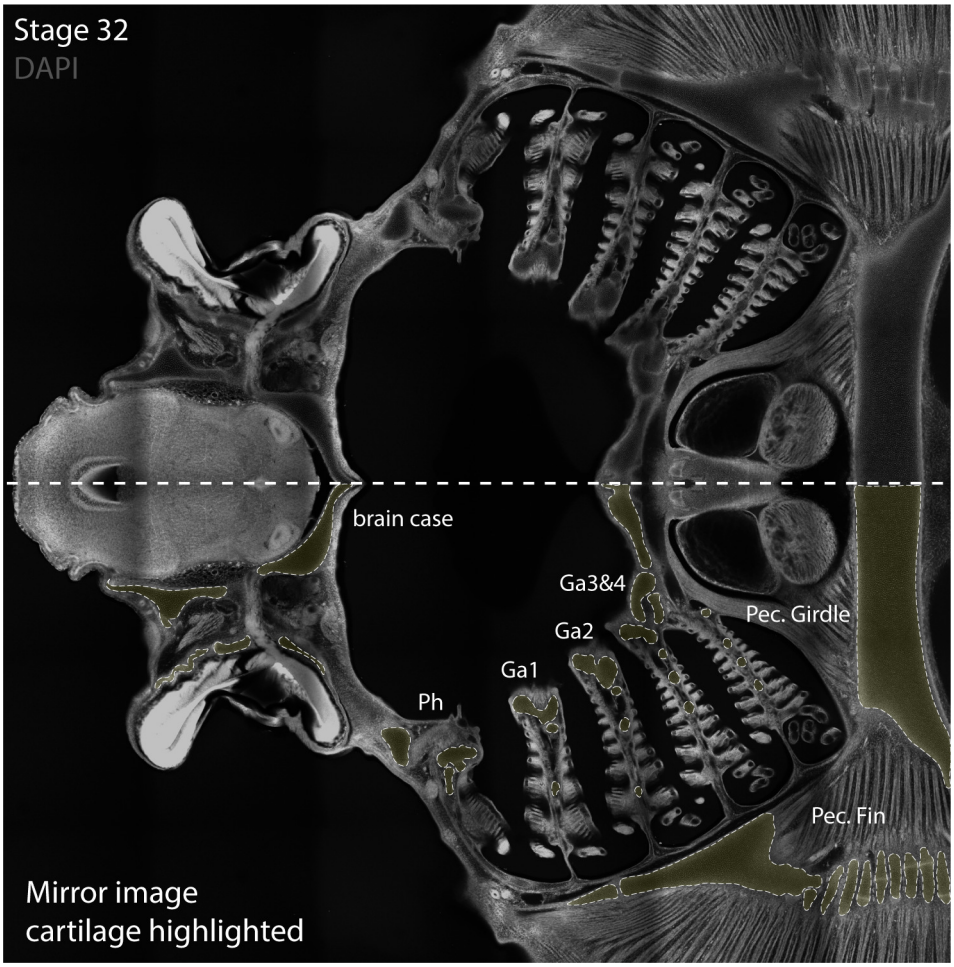

Figure 2—figure supplement 1. Identification of skate pharyngeal arch skeletal elements in section. Cartilaginous elements of the pharyngeal skeleton of a S32 skate embryos are readily visible in DAPI-stained sections, as shown here without (top) and with false-colouring of cartilages in yellow (bottom).

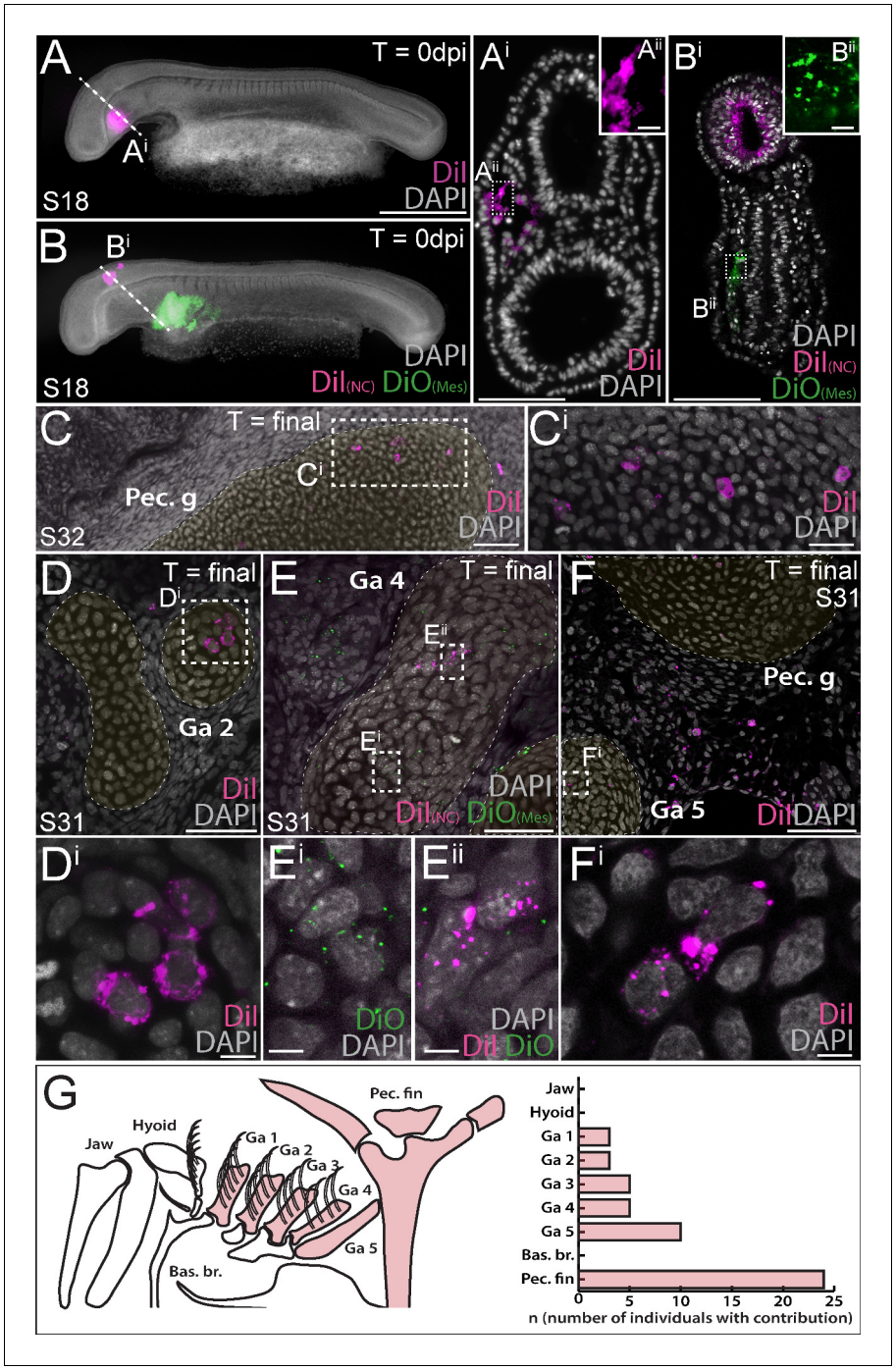

Figure 3. Mesoderm contributes to the gill arch and pectoral fin skeleton in the skate. (**A, A^{i}**) Microinjection of CM-DiI into the head mesoderm (HM) of a skate embryo at S18. (**B, B^{i}**) Simultaneous labelling of the hindbrain neural tube (including premigratory cranial neural crest cells) with CM-DiI and lateral plate mesoderm (LPM) with SpDiOC$_{18}$ in a S18 skate embryo. (**C, C^{i}**) LPM gives rise to chondrocytes within the skeleton of the pectoral fin and girdle, while mesoderm at the HM-LPM boundary and LPM give rise to chondrocytes within the gill arch skeleton – e.g. (**D, D^{i}**) in the branchial rays of gill arch 2. (**E**) After double labelling of the LPM with SpDiOC$_{18}$ and the neural tube with CM-DiI, as in (**B**) above, both (**Ei**) SpDiOC$_{18}$- and (**Eii**) CM-DiI-labelled chondrocytes are recovered within the gill arch skeleton – for example, in the ceratobranchial of gill arch 4 – demonstrating the dual mesodermal and neural crest origin of these elements. (**F, F^{i}**) Mesodermally-derived chondrocytes were also recovered in the ceratobranchial of gill arch 5, in close proximity to the label-retaining pectoral girdle and surrounding connective tissue. (**G**) Schematic summary of pharyngeal and paired fin skeletal elements in the S32 skate embryo, with

Figure 3 continued on next page

Figure 3 continued

elements receiving any mesodermal contributions (HM, HM-LPM or LPM) coloured red, and a plot showing the number of embryos observed with mesoderm contributions to the pharyngeal arch and pectoral fin skeleton. In (**D**), (**E**) and (**F**), cartilaginous elements are false-coloured yellow. Scale bars: A, B = 700 μm; A^{i} = 125 μm; A^{ii} = 15 μm; B^{i} = 50 μm; B^{ii} = 15 μm; C = 60 μm; C^{i} = 20 μm; D = 50 μm; D^{i} = 5 μm; E = 30 μm; E^{i} = 5 μm; F = 60 μm; F^{i} = 7 μm.

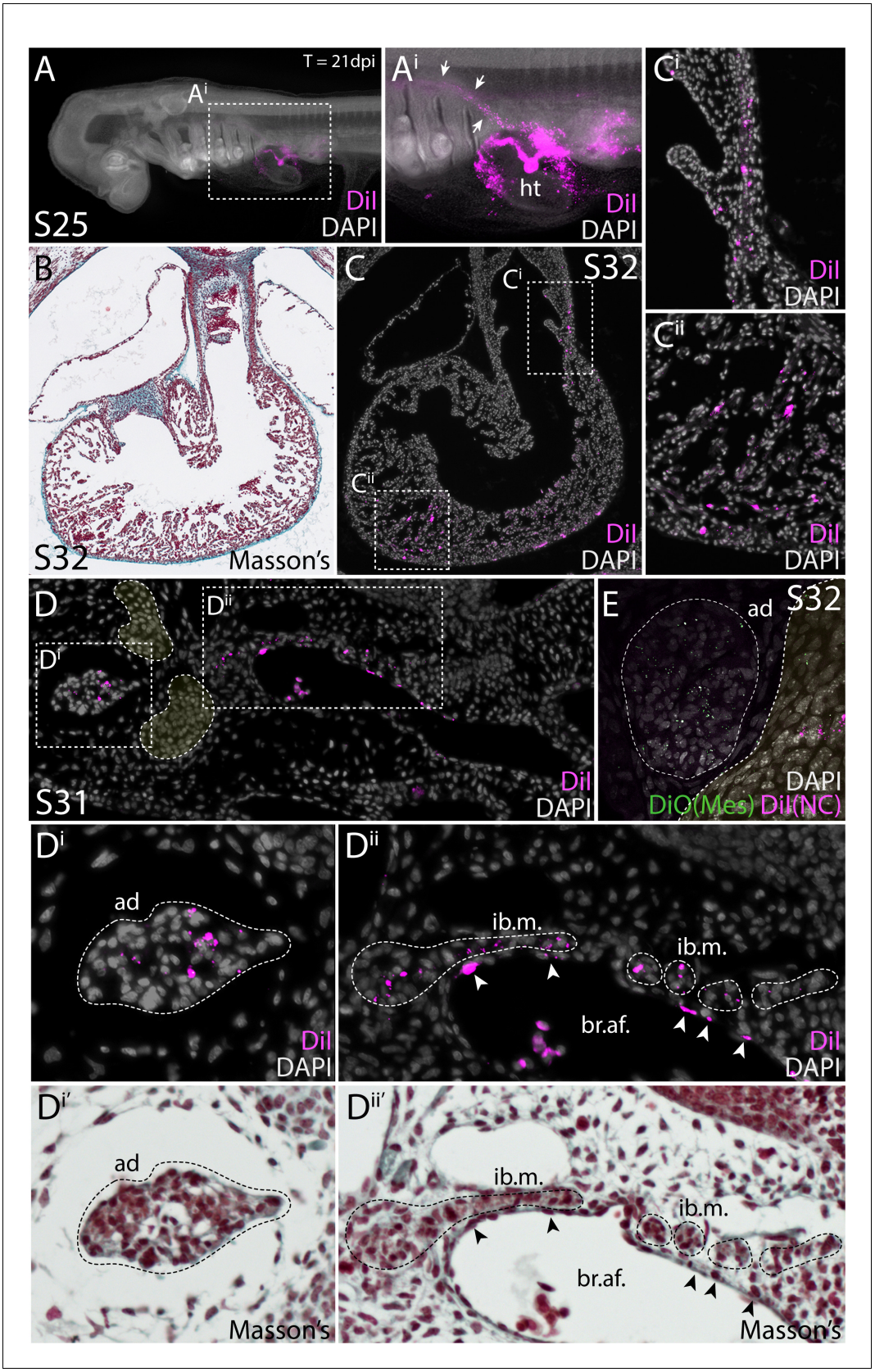

Figure 3—figure supplement 1. Cardiopharyngeal mesodermal derivatives in the skate. (**A**) A skate embryo 21 days after CM-DiI labelling of lateral mesoderm at the HM-LPM boundary. Abundant label is recovered within the heart (ht) and major blood vessels (white arrows in **A**^{i}). (**B**) Histological

Figure 3—figure supplement 1 continued on next page

Figure 3—figure supplement 1 continued

section through the heart of a S32 skate embryo, stained with Masson's trichrome. (**C**) Adjacent section to (**B**), showing labelling of the heart after CM-DiI injection in lateral mesoderm of the HM-LPM boundary. (**D**) Example of branchiomeric musculature (branchial adductor muscle, *ad*, and interbranchial musculature, *ib.m.*) and vascular endothelium (white arrowheads) derived from lateral mesoderm (**D**$^{i'}$ and **D**$^{ii'}$) are the same sections as (**D**^{i} and **D**^{ii}), respectively, imaged after Masson's trichrome counterstaining. Condensing gill arch cartilage is false coloured in yellow. (**E**) SpDiOC$_{18}$ labelling of branchiomeric musculature (branchial adductor muscle, *ad*) reveals its mesodermal origin, from an embryo in which lateral mesoderm was labelled with SpDiOC$_{18}$ and the neural tube was labelled with CM-DiI at S18.

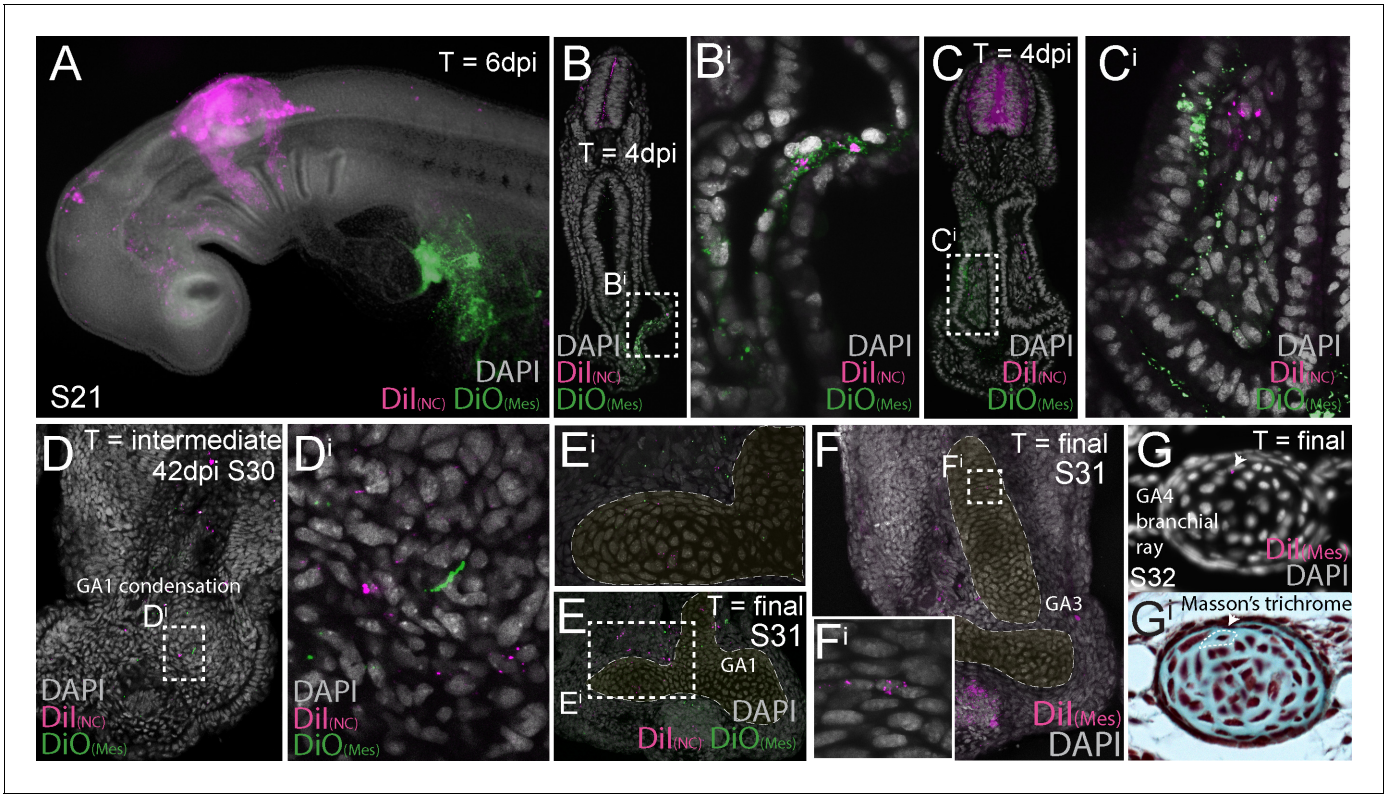

Figure 3—figure supplement 2. Dual embryonic neural crest and mesodermal origin of gill arch cartilages in the skate. (**A**) A skate embryos 6 days after neural tube labelling with CM-DiI and lateral plate mesoderm (LPM) labelling with SpDiOC$_{18}$. (**B–C**) Transverse sections reveal that 4 days post neural tube labelling with CM-DiI and LPM labelling with SpDiOC$_{18}$, CM-DiI-labelled neural crest cells can be seen migrating adjacent to SpDiOC$_{18}$-labelled LPM. (**D**) Forty-two days post-dual labelling, both CM-DiI-retaining (i.e. neural crest-derived) and SpDiOC$_{18}$-retaining (i.e. LPM-derived) cells are recovered within the condensing ceratobranchial cartilage of gill arch 1, while (**E**) at S32, CM-DiI-retaining and SpDiOC$_{18}$-retaining chondrocytes are recovered within the ceratobranchial cartilage of gill arch 1. (**F**) Mesodermal contribution to the ceratobranchial cartilage of gill arch 3. (**G**) Mesodermal contribution to a branchial ray on gill arch 4. In (**E**) and (**F**), cartilaginous elements are false-coloured yellow.

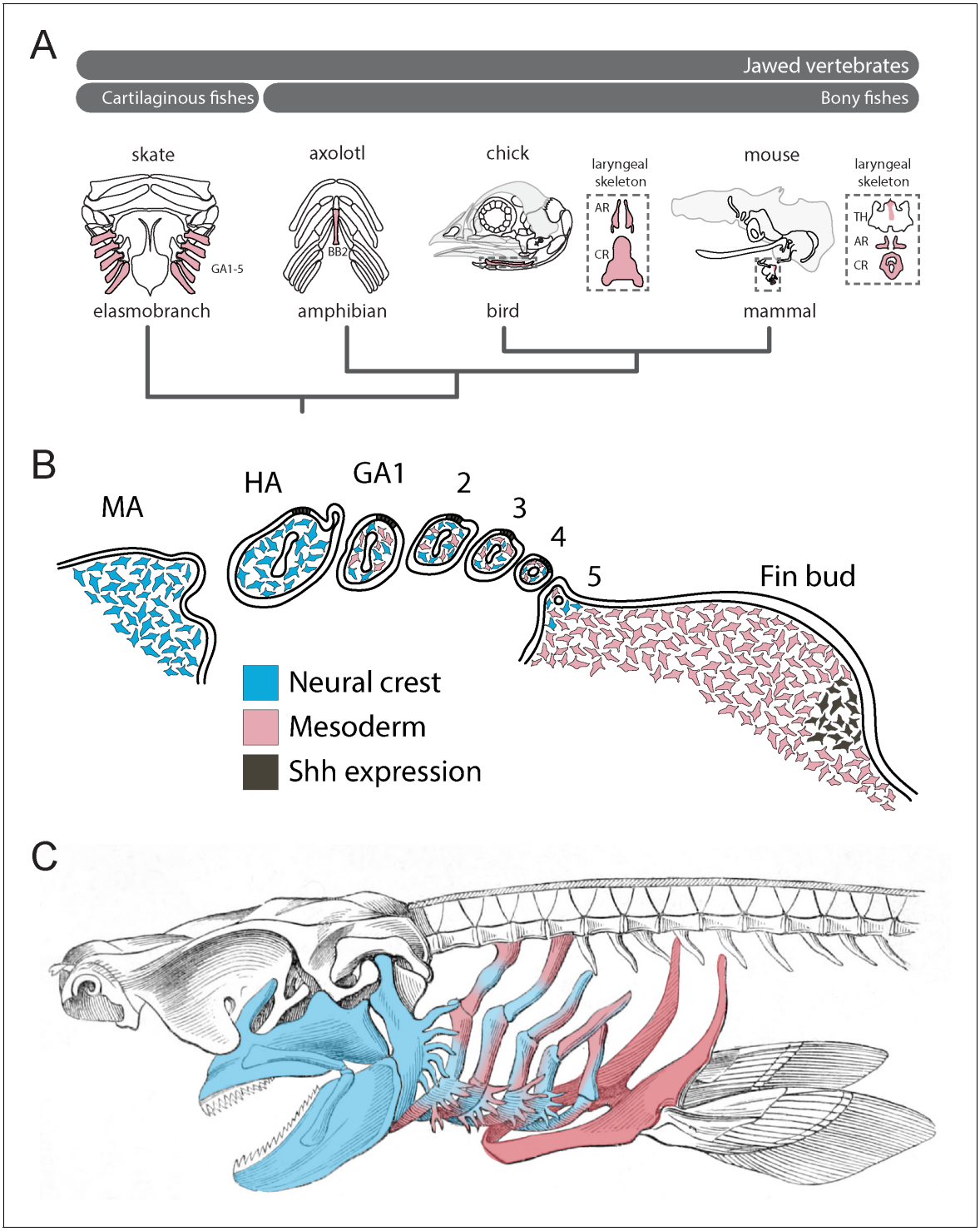

Figure 4. Mesodermal contributions to the pharyngeal endoskeleton in jawed vertebrates. (**A**) Mesodermal contributions (red) to the gill arch skeleton in skate, the basibranchial skeleton in axolotl and the laryngeal skeleton of chick and mouse points to an ancestral mesodermal contribution to the pharyngeal arch skeleton of jawed vertebrates. (**B**) Schematic representation of neural crest- (blue) and mesoderm-derived (red) skeletogenic mesenchyme in the skate pharyngeal arches and pectoral fin bud, in relation to epithelial and mesenchymal *Shh* expression, respectively. (**C**) We propose that the mandibular and hyoid arch skeleton are neural crest-derived and the pectoral fin skeleton mesodermal derived, while the gill arch skeletal elements are of dual neural crest and mesodermal origin.